JCBI
Journal of Computing & Biomedical Informatics
ISSN: 2710 - 1606
Volume 09 Issue 02
2025

Research Article
https://doi.org/10.56979/902/2025

Lung Cancer Classification through Transfer Learning and Deep Feature Extraction using EfficientNetB3

Muhammad Usama Naveed[1], Muhammad Munwar Iqbal[1], Saqib Majeed[2], Farooq Ali[1], and Qamas Gul Khan Safi[1]

[1]Department of Computer Science, University of Engineering and Technology, Taxila, Pakistan.
[2]University Institute of Information Technology, PMAS Arid Agriculture University, Rawalpindi, Pakistan.
Corresponding Author: Muhammad Munwar Iqbal. Email: munwar.iq@uettaxila.edu.pk

Received: July 03, 2025 **Accepted**: August 15, 2025

Abstract: Worldwide, lung cancer is one of the deadliest diseases. It is critical to make an early diagnosis of lung cancer for treatment. The standard process of diagnosis by a pathologist is by examining the histopathology images. The assessment of images by a pathologist is still prone to errors and time-consuming. To enhance the speed of the entire process and to accurately diagnose cancer in images, an automated procedure of cancer diagnosis is essential. In this paper, an automated process for lung cancer classification is proposed by using a pretrained deep model, EfficientNetB3. The proposed scheme uses lung cancer histopathological images, which are obtained from the 'LC25000' dataset. During the preprocessing phase, images were resized to a fixed dimension of 224x224x3 pixels. EfficientNetB3 was trained over 15,000 images of lung cancer classes, including squamous cell carcinoma, adenocarcinoma, and benign. After transfer learning, features are extracted from the model's second-to-last layer, or the dropout layer, which has an Nx512 dimension. The classifiers are then fed the feature vector as input to classify lung cancer after it has been divided into 80%, 10%, and 10% for training, validation, and testing. The proposed methodology is evaluated by different performance metrics, i.e., accuracy, recall, precision, FNR, TNR, FPR, F1-score, and misclassification rate. The results show that achieved the highest accuracy of 0.9980 with a misclassification rate of 0.0020, which was achieved by the proposed technique for Bilayered NN, which represents an improvement over the state-of-the-art techniques.

Keywords: Lung Cancer; CNN; Histopathology Images; Transfer Learning; Classification; Pathologist

1. Introduction

Lung cancer is one of the most prevalent and significant causes of death globally. While the primary cause of lung cancer is smoking cigarettes, other factors that may contribute to the disease include being overweight, eating red and processed meat, drinking alcohol, not eating enough fruits and vegetables, or being exposed to UV radiation [1]. As per GLOBOCAN statistics of 2020, Worldwide an estimate of 19.3 million cases of cancer were registered, where 2,206,771 new cases were reported, from which 1,796,144 were reported dead from lung cancer [2]. According to the WHO (World Health Organization) statistics for the United States of 2023, 62,000 deaths were caused by lung cancer [3]. In 2025, statistics show that the total estimated new cases registered were 226,650, of which 124,730 were reported dead in the United States [4] which shows a significant increase in the mortality rate.

Histopathological imaging analysis is one of the most superior standards for the diagnosis of cancer, allowing precise tumor classification and grading. Lung cancer in early stages often does not exhibit any symptoms or signs of illness, despite potentially having a disease or medical condition, which limits the treatment options [6]. According to studies, it is reported that the survival rate decreases approximately

17% in the case of advanced stages of lung cancer; however, the survival rate increases up to 50% upon early stage detection [7].

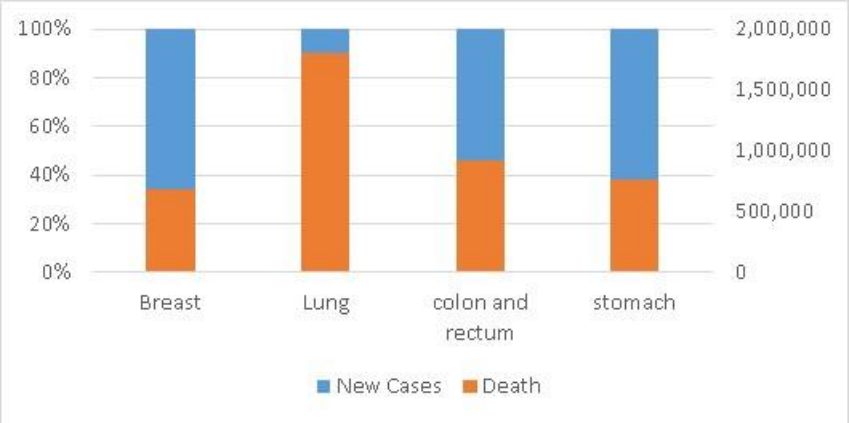

Figure 1. Graph 1 - Worldwide Cancer Cases and Deaths in 2020 [5]

ML [Machine Learning] and DL [Deep Learning] are revolutionizing diagnostic capabilities by processing medical images. ML algorithms that have been trained on large histopathological imaging datasets can detect cancerous characteristics rapidly, increasing the diagnostic time and detection [8]. Likewise, DL algorithms applied to histopathological imaging show accuracy that is close to or better than humans, improving the diagnostic reliability and consistency [9].

A subset of DL called Convolutional Neural Networks (CNNs) has demonstrated impressive results on deciphering intricate patterns found in histopathological imaging, which is essential for precise categorization. Like MobileNet [10], DenseNet [11], GoogLeNet [12], VGG [13], AlexNet [14] and more, are the range of CNN architectures that have been applied and effectively used on medical imaging [15]. These models can be used for extracting deep features to help ML classifiers categorize more effectively.

The ability of EfficientNetB3 to achieve an equilibrium between accuracy and computing efficiency has made it a particularly successful technique. Because of its depth and optimized width, its architecture can operate at high speed with relatively low computing expenses [16]. Compared to other DL models, EfficientNetB3 is a perfect option for medical imaging categorization, where efficiency, scalability, and ease of use are the most important factors to speed up the diagnostic process. In order to maintain computational viability without compromising accuracy, we used EfficientNet-B3, which provides a better accuracy and efficiency trade-off than MobileNetV2 and DenseNet201. We also resized the 768×768 histopathology patches to 224×224 (with normalization) to match ImageNet pretraining.

Despite advances in digital pathology and imaging, distinguishing between cancerous and non-cancerous cells remains an issue due to subtle morphological differences and tumor heterogeneity. This paper aims to increase the Lung cancer classification using the histopathological medical imaging by extracting the deep feature using EfficientNetB3 and passing it on to ML classifiers, for accurate classification. This study uses the histopathological images from LC25000 dataset [17], which is publicly available and has cancer classes for colon and lung. However, we only aim to improve the classification of lung cancer, which is composed of 15000 images from the total dataset.

This paper follows the following structure: Section 2 shows the previous related work done; Section 3 demonstrates and describes the proposed technique and helps understand the mathematical calculation used by the model architecture; Section 4 discusses and evaluates the performance of the models used in the proposed methodology and shows the numerical statistics; and Section 5 concludes the paper with final comments.

2. Literature Review

In recent years, Deep Learning has evolved as a leading approach in medical imaging analysis. This approach has optimized the conventional way of extracting features from images. Anjum, S., *et al.* [18] proposed a lung cancer classification technique by using multiresolution EfficientNet variants. In the proposed technique, all EfficientNet variants, i.e., B0 to B7, are transfer learned to compare their

performance. The dataset used in this paper was LC25000, which includes different types of cancers for the lung and colon. During the transfer learning process for each EfficientNet variant, different image resolutions were selected and evaluated accordingly. The EfficientNetB2 variant results show that the highest accuracy of about 97% for a 260x260 pixel image resolution.

Li, M., *et al.* [19] This study shows the diagnosis and classification of lung cancer subtypes using the multi-dimensional features extracted. In this study, SVM was trained using these features. The study's dataset was obtained clinically from a Xinjiang cancer hospital. Samples from 94 patients with lung cancer are included in this dataset. According to the experimental results shown, the Relief-SVM model exhibits the best classification results. Specifically, the acquired accuracy for ASC-SCLC, LUSC-ASC, and LUSC-SCLC was 73.67%, 73.91%, and 83.91%, respectively.

A Lung and colon classification technique by using the CNN models was proposed by Singh, O., et al. [20]. Multiple pre-trained CNN models, including MobileNetV2, EfficientNetB6, InceptionResNetV2, VGG19, and DenseNet201, were used for the lung and colon cancer sub-classes classification. The LC25000 was used as a dataset to validate the pre-trained CNN model's performance. The experimental process, shows that MobileNetV2, EfficientNetB6, InceptionResNetV2, VGG19 and DenseNet201 achieved accuracy of about 99.32%, 93.12%, 97.92%, 98%, and 99.12% respectively.

Mahmud, M. R., et al. [21] proposed a histopathological and computed tomography imaging-based hybrid deep learning approach to recognize lung cancer. Multi-stage preprocessing was applied in order to enhance image quality by resizing, noise reduction, and normalization. To resolve the issue of class imbalance, augmentation was applied, which improved generalization. A hybrid LEViT model was proposed, which was based on ViTs and CNNs models to provide a high-speed, lightweight, and robust framework for lung cancer classification [22]. The proposed method was evaluated using 10-fold cross-validation. LEViT outperformed and gave an accuracy of about 99.43% on IQ-OTH/NCCD and 99.02% on the LC25000 dataset.

An attention-based technique by using the CNN-based DenseNet model is proposed by Uddin, J. J. D. et al. [23] for the lung cancer classification. The dataset used in this study consisted of two types of medical imaging, i.e., computed tomography and histopathological, where 340 and 15000 images were used, respectively. The DenseNet used has the capability to transmit through each layer the learned features, improving local feature learning while reducing the model's parameters. Moreover, an attention mechanism was incorporated, which helps the model to focus on more relevant regions. ATT-DenseNet demonstrated an impressive accuracy of 95.4% and 94% over the histopathological and CT scans images, respectively.

In the domain of digital pathology, CNNs plays a significant role for analysis of medical imaging and have efficiently extracted features that are far superior to the traditional handcrafted features. Kumar, A., et al. [24] introduces a ML3CNet [Multi-headed Lung Cancer Classification Convolution Neural Network]. In this work, noise has been removed from the photos while maintaining the edges of the images using a non-local mean [NLM] filter. Histopathological images of lung cancer which has three different types form the basis of the dataset. The accuracy of the suggested model is 98.92%.

A computer-aided diagnosis [CAD] based technique for the diagnosis of lung cancer was proposed by Li, Z., et al. [25]. Pixel-wise cancer detection in whole-slide imaging was the main focus of this study's suggested Automatic cancer detection and classification in while-slide lung histopathology (ACDC@LungHP). Histopathological images of 200 lung cancer patients from the First Hospital of Changsha were collected for the dataset, where 150 of these cases were used for training, and 50 for testing. Multi-Model, which was based on the Otsu algorithm, obtained the greatest accuracy of 0.9508, according to the test set findings.

TL [Transfer Learning] has emerged as a significant method in deep learning, as it allows the model to learn hidden patterns from less data, which has major significance in the field of medical images. Nafea, A. A., et al. [26] proposed a TL-based technique for lung cancer classification by using a pretrained EfficientNetB3 model. The dataset used in the study is based on computed tomography images of the human chest, which were gathered from Kaggle. The dataset consists of 1000 scan images, which were obtained from different patients with different respiratory conditions. For training, validation, and testing, the dataset was split into 613, 315, and 72 images, respectively. EfficientNetB3 outperformed in this study, with an accuracy of 96%.

3. Proposed Methodology

In this section, the proposed methodology, along with its detailed flow, is explained. We used only 3 classes from the LC25000 dataset pertaining to lung only, which was resized to 224x224. The EfficientNet-B3 model was trained using transfer learning for lung cancer classification, and the deep features were extracted from the second last layer, i.e., dropout layer. The extracted features are divided into an 80%, 10%, 10% ratio, which is training, validation, and testing. Then, we trained the classifiers from different families and compared the results for the models trained. The proposed methodology used in this paper is shown in Figure .

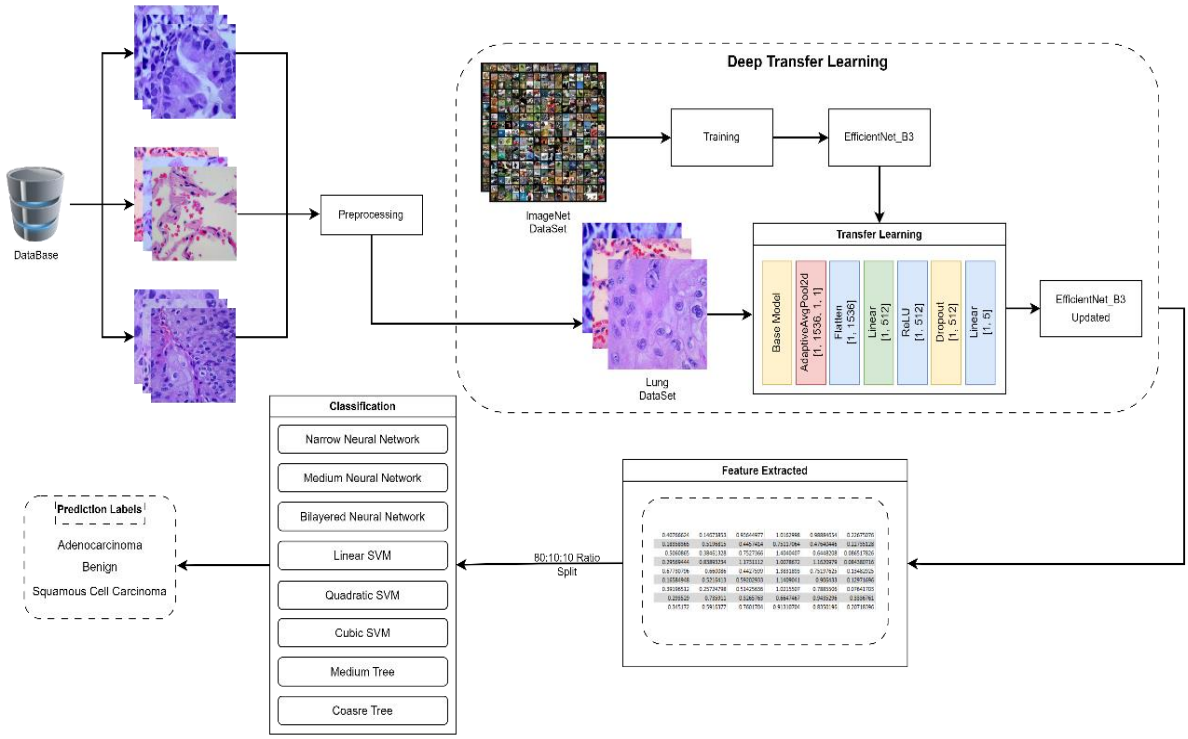

Figure 2. Proposed Methodology

3.1. DataSet Preparation

The dataset of histopathological lung images serves as the primary dataset, sourced from Kaggle and publicly available. These images are obtained from original, validated, and HIPAA-compliant sources, which had 750 images, consisting of 250 for each class, i.e., Adenocarcinoma, Benign, and Squamous Cell Carcinoma [17]. Then these 250 images of each class are augmented to generate 5000 images for each class, which is a total of 15,000 images. Figure shows a few images as a sample for the dataset classes. Whereas, the breakdown of dataset classes is listed in Table.

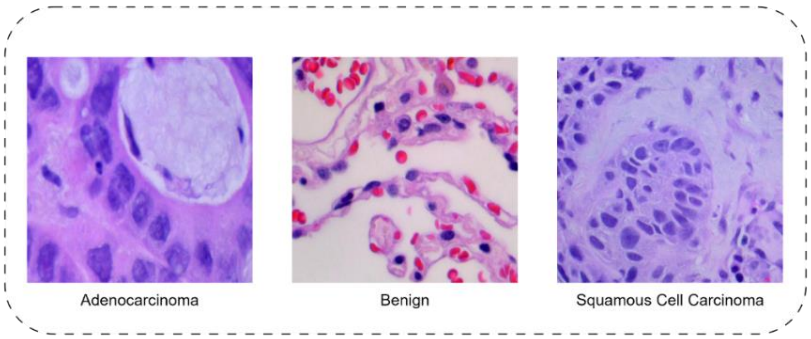

Figure 3. Sample Images of Dataset Classes

Table 1. Breakdown of Dataset Classes

Class	Database Name	Total Images
Adenocarcinoma	LC25000 [only Lung excluding colon]	5000
Benign		5000
Squamous Cell Carcinoma		5000

These images are then resized to a fixed dimension of 224x224x3 pixels to match the input dimension required by EfficientNetB3 Model. Here, each image I is represented as:

$$I \in \mathbb{R}^{224x224x3}$$

3.2. EfficientNet-B3 Deep Model

In recent years, Deep Neural Networks have made substantial advancements in the field of image classification. By definition, a deep model is a blend of low-level, mid-level, and high-level features along with a classifier. In this paper, we have used EfficientNet-B3 to extract deep features. The pretrained model used is basically trained on ImageNet [27] and is used as the convolutional backbone with all its parameters frozen. This model, used as a convolution backbone, consists of Conv / Stem Layers and MBConv [Mobile Inverted Bottleneck Convolution] Blocks with progressive down-sampling. At the output of the final MBConv block, the features tensor has a shape, represented as:

$$T \in \mathbb{R}^{7x7x1536}$$

3.3. Network Training based on Transfer Learning

In deep learning, the reliance on large datasets is a significant challenge. Compared to a typical Machine Learning model, the DL models require a substantially larger volume of data for effective training. The requirement of this large volume of data is to uncover complex, hidden patterns. However, in some domains like medical imaging, acquiring a large volume of data can be difficult. To address this issue, Transfer learning is used to train a model on smaller datasets [28]. Though transfer learning is not required to train the model from scratch, as the knowledge base from the source domain can be leveraged to improve the performance on the target task.

Transfer Learning is mathematically defined using a domain$H = [Y, P[Y]]$, where $Y$the feature is space and $P[Y]$ is its probability distribution. For a task $L = [J, h[.]]$ which consists of label space, i.e., J and a predictive function, i.e., $h[.]$ which is learned from the pair of labels, i.e., $[y_i, j_i]$. Here, the source and target domains are represented by H_S andH_T, along with their respective predictive function, i.e., $h_S[.]$ and $h_T[.]$. TL aims to improve the $h_T[.]$ using the knowledge base from the H_S and its tasks, even when$H_S \neq H_T$.

Figure shows the model learning process using transfer learning.

3.1.1. Custom Layer

To adapt for the target classification task, a custom classification head was appended after the convolutional backbone with all its parameters frozen.

1. Adaptive Average Pooling converts the 7x7x1536 to 1x1x1536 by averaging over spatial dimensions, which is formulated as represented below in :

$$h_c = \frac{1}{H\ X\ W} \sum_{i=1}^{H} \sum_{j=1}^{W} T_{i,j,c} \quad (1)$$

2. Flatten Layer reshapes the 1x1x1536 to a vector, which is mathematically represented below. This vector basically represents the features before the custom added fully connected layer.

$$z \in \mathbb{R}^{1536}$$

3. Fully Connected Layer [FC1] reduces dimensionality from 1536→512. Where 'σ' is the ReLU activation function in equation [2].

$$h = \sigma(W_1 z + b_1),\ W_1 \in \mathbb{R}^{512\ X\ 1536} \quad (2)$$

4. Dropout Layer randomly zeroes 30% of the activations to prevent overfitting.
5. Fully Connected Layer [FC2] maps 512→K [where K is the number of classes] followed by softmax during classification.

$$\hat{y} = Softmax[W_2 h' + b_2] \quad (3)$$

After training, the penultimate layer i.e., dropout layer output [$z \in \mathbb{R}^{512}$] was extracted as the deep feature vector for each image. For N total images, the final feature matrix is:

$$Z = \begin{bmatrix} Z_1^T \\ Z_2^T \\ \vdots \\ Z_N^T \end{bmatrix} \in \mathbb{R}^{N\ X\ 512} \quad (4)$$

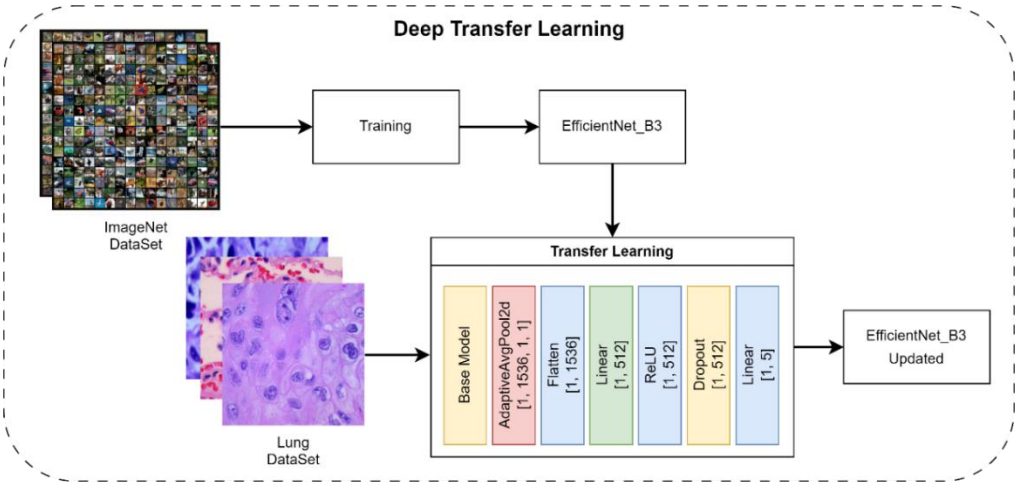

Figure 4. Deep Transfer Learning

The optimization was performed by following the parameter configuration as listed in Table 1.

Table 1. Hyperparameters configurations

Hyper parameters	Configuration
Optimizer	Adam
Loss Function	Cross Entropy
Learning Rate	0.0001
Epochs	20

3.4. Classification

The features extracted with shape Nx512 are stored in the CSV format for reuse for multiple classifiers without repeating the extraction steps. Before training the classifiers, the features were split into 80% training, 10% validation, and 10% testing, which is shown in Table 2 using stratified random splits with a fixed random seed [42], ensuring class balance and reproducibility. Only the validation set [10%] was used for model selection and hyperparameter tuning. Multiple classification models were used from different families, including NN, SVM, and DT.

Table 2. Training, Validation, and Testing Splits

Splits	Ratio	No. of Images
Training	80	12000
Validation	10	1500
Testing	10	1500

Categorical cross-entropy loss and the Adam optimizer [learning rate = 0.001] were used to train the neural networks across 10 epochs with a batch size of 32. The narrow NN used one hidden layer with 32 ReLU units, the medium NN used two hidden layers with 64 and 32 units, and the bilayered NN used two hidden layers with 128 and 64 units. With probability outputs enabled, the SVM models comprised a cubic SVM [polynomial kernel, degree=3, C=1.0, gamma=scale], a quadratic SVM [polynomial kernel, degree=2, C=1.0, gamma=scale], and a linear SVM [kernel=linear, C=1.0, probability=True]. Using the Gini criterion and the default scikit-learn parameters, the decision tree models included a medium tree with a maximum depth of 10 and a coarse tree without any depth restrictions. Moreover, the Table 3 shows the summary of the hyperparameters used by each classifier.

Table 3. Summary of hyperparameters used in classifiers

Classifier	Architecture / Kernel	Key Hyperparameters
Narrow NN	1 hidden layer [32]	Optimizer = Adam [lr=0.001] Loss = CE Activation = ReLU Batch_Size = 32 Epochs = 10
Medium NN	2 hidden layers [64 → 32]	Optimizer = Adam [lr=0.001] Loss = CE Activation = ReLU Batch_Size = 32 Epochs = 10
Bilayered NN	2 hidden layers [128 → 64]	Optimizer = Adam [lr=0.001] Loss = CE Activation = ReLU Batch_Size = 32 Epochs = 10
Linear SVM	Linear kernel	C=1.0 Shrinking=True Probability=True Gamma=scale
Quadratic SVM	Polynomial kernel [deg=2]	C=1.0 Coef0=0.0 Probability=True Gamma=scale
Cubic SVM	Polynomial kernel [deg=3]	C=1.0 Coef0=0.0 Probability=True
Medium Tree	Decision Tree [depth=10]	Criterion=gini Min_samples_leaf=1 Min_samples_split=2 Splitter=best
Coarse Tree	Decision Tree [no depth limit]	Criterion=gini Min_samples_leaf=1 Min_samples_split=2 Splitter=best

4. Experimental Analysis

For obtaining the results for our experimentation, we used Intel Core i5 12th generation with 32 GB RAM and Windows 11 Pro as the OS. The environment used for the simulation and obtaining results was Python, along with Jupyter Notebook.

This section provides a detailed discussion of the statistical results we have obtained. The dataset used for our experimentation was LC25000, where classes related to Lung Cancer were used. Originally, the LC25000 dataset had 25000 images, where 2 classes were for colon and 3 classes were for lungs, and each class had 5000 images. However, in our case, we only use the lung cancer classes, which were Adenocarcinoma, Benign, and Squamous Cell Carcinoma, with a total of 15000 images.

In preprocessing, we resized the images from each class to a fixed dimension, i.e., 224x224, and performed normalization. After the preprocessing, the total of 15000 images from 3 classes of lungs were passed to the deep model, i.e., EfficientNet-B3, which was used to obtain deep features by transfer learning. The deep features after transfer learning were obtained from the second last layer, i.e., dropout layer of the model, and were saved, split into an 80%, 10% and 10% ratio, which is training, validation, and testing, respectively. Figure shows the training loss and accuracy for the EfficientNet-B3.

After the feature extraction, multiple classifiers were utilized to compare the accuracies. The classifiers used are Narrow NN, Medium NN, Bilayered NN, linear SVM, cubic SVM, Quadratic SVM, Medium SVM, coarse tree, and medium tree. Various performance metrics were used to report the results, such as accuracy, recall, specificity [TNR], F1-score, precision, misclassification rate, FPR [False Positive Rate], and FNR [False Negative Rate], where all of these are calculated by the formula as follows in equations [1] to [8]:

$$Accuracy = \frac{TP + TN}{TP + TN + FN + FP} \quad (5)$$

$$Recall = \frac{TP}{TP + FN} \quad (6)$$

$$Precision = \frac{TP}{TP + FP} \quad (7)$$

$$F1 - Score = \frac{2 \times Precision \times Recall}{Precision + Recall} \quad (8)$$

$$Specificity = \frac{TN}{TN + FP} \quad (9)$$

$$FPR = 1 - Specificity \quad (10)$$

$$FNR = 1 - Recall \quad (11)$$

$$Misclassification\ Rate = 1 - Accuracy \quad (12)$$

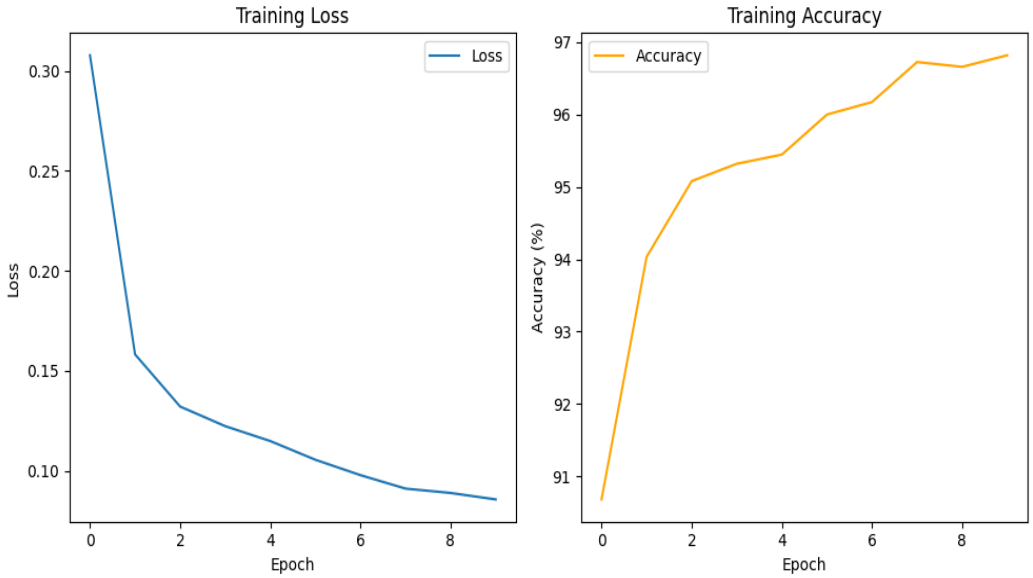

Figure 5. EfficientNet-B3 Training Loss and Accuracy

Here, TP = True Positive, TN = True Negative, FP = False Positive, FN = False Negative.

4.1. Bilayered Neural Network

Figure shows the accuracy and loss for both the training and validation phases. Whereas, Figure shows the confusion matrix, and to complement the confusion matrix Figure shows the ROC-AUC curve and Table 4 shows the class-wise classification report for the best classifier, i.e., Bilayered Neural Network.

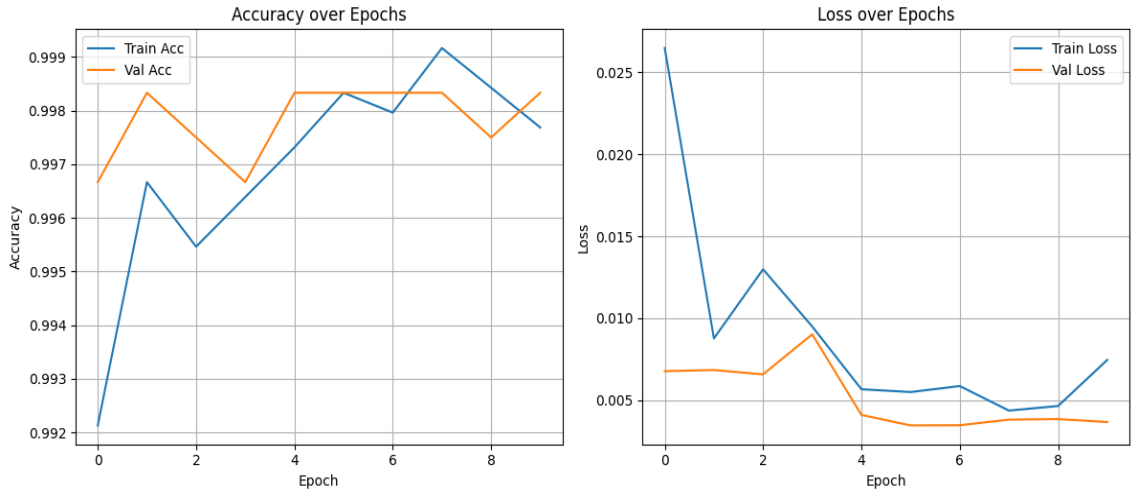

Figure 6. Bilayered Neural Network Training Loss and Accuracy

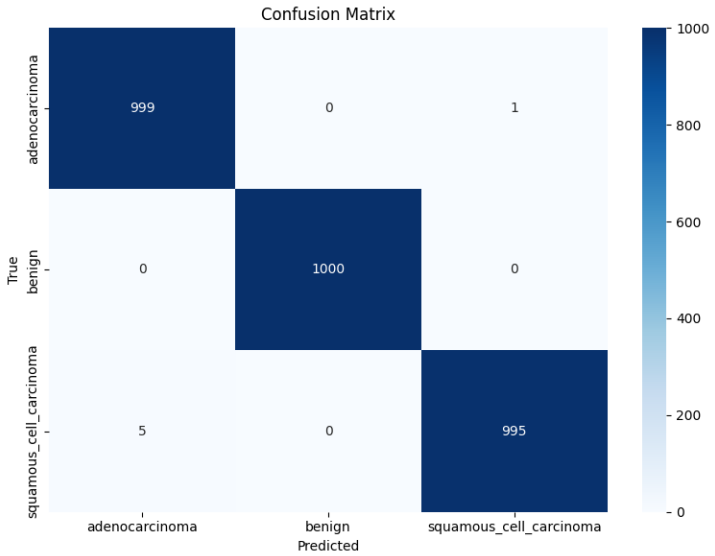

Figure 7. Bilayered Neural Network Confusion Matrix

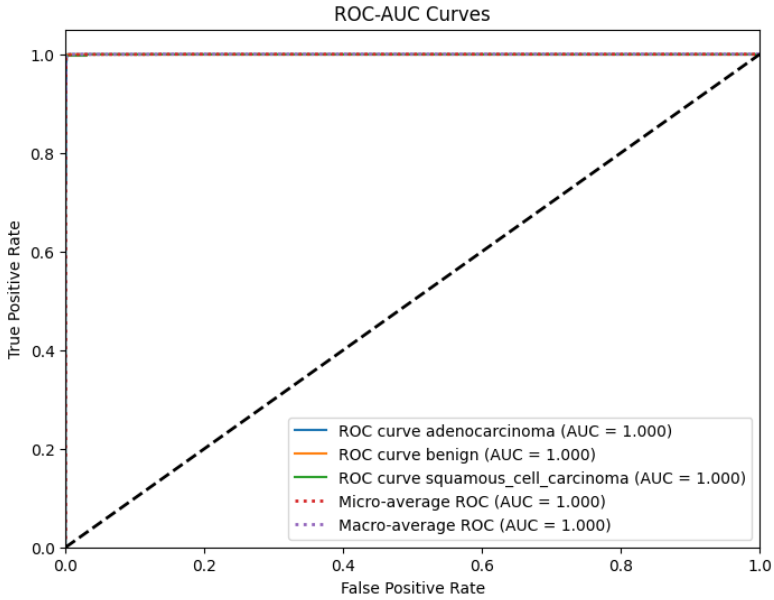

Figure 8. Bilayered Neural Networks ROC-AUC Curves

Table 4. Bilayered Neural Network Classification Report

Class Name	Precision	1-Precision	Recall	F1 score
Adenocarcinoma	0.9950	0.0050	0.9990	0.9970
Benign	1.0000	0.0000	1.0000	1.0000
Squamous Cell Carcinoma	0.9990	0.0010	0.9950	0.9970

5. Results

This section shows the numerical results from our experimentation. Bilayered NN produced the best results out of all the classifiers, with an accuracy of 0.9980, precision, recall, and F1-score of 0.9980, and a misclassification rate of 0.0020, as shown in Table . As the LC25000 dataset has balanced classes, the micro and macro average scores may coincide, which is why the precision, accuracy, F1 score, and recall values are reported as identical. Figure 9. **Graph 2** shows the visualization of numerical results along with the misclassification rate.

Table 6. Results from Classifiers

Classifiers	Accuracy	Precision	Recall	F1-Score	Misclassification rate	CI
Narrow NN	0.9970	0.9970	0.9970	0.9970	0.0030	0.997 [0.995 – 0.998]
Medium NN	0.9970	0.9970	0.9970	0.9970	0.0030	0.997 [0.995 – 0.998]
Coarse Tree	0.9817	0.9817	0.9817	0.9817	0.0183	0.9817 [0.9797 – 0.9837]
Linear SVM	0.9957	0.9957	0.9957	0.9957	0.0043	0.9957 [0.9937 – 0.9977]
Quadratic SVM	0.9967	0.9967	0.9967	0.9967	0.0033	0.9967 [0.9947 – 0.9987]
Cubic SVM	0.9950	0.9950	0.9950	0.9950	0.0050	0.995 [0.993 – 0.997]
Medium Tree	0.9857	0.9857	0.9857	0.9857	0.0143	0.9857 [0.9837 – 0.9877]
Bilayered NN	**0.9980**	**0.9980**	**0.9980**	**0.9980**	**0.0020**	**0.998 [0.996 – 0.999]**

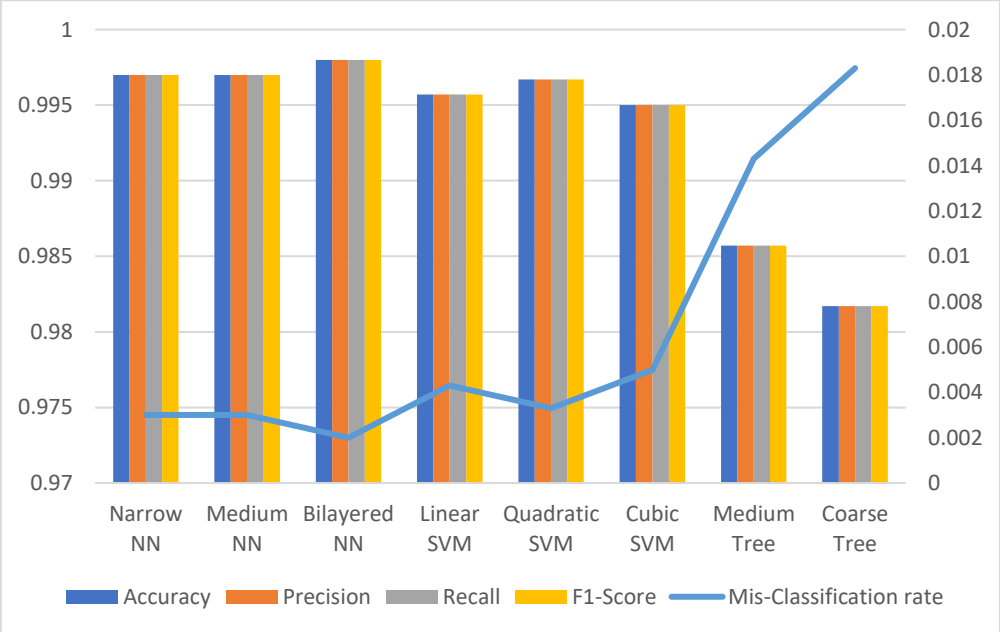

Figure 9. Graph 2 - Visualization of Numerical Results Along with Misclassification Rate

Moreover, the class-wise True Negative Rate [TNR], False Negative Rate [FNR], and False Positive Rate [FPR] for the classifiers are detailed in the Table 5.

Table 5. Class-wise TNR, FNR, and FPR for classifiers

Classes / Classifiers	Adenocarcinoma			Benign			Squamous Cell Carcinoma		
	TNR	**FNR**	**FPR**	**TNR**	**FNR**	**FPR**	**TNR**	**FNR**	**FPR**
Narrow NN	0.9975	0.0039	0.0025	1.0000	0.0000	0.0000	0.9955	0.0050	0.0020
Medium NN	0.9990	0.0068	0.0010	1.0000	0.0000	0.0000	0.9965	0.0020	0.0035
Coarse Tree	0.9862	0.0270	0.0138	0.9995	0.0021	0.0005	0.9865	0.0252	0.0135
Linear SVM	0.9964	0.0058	0.0036	1.0000	0.0000	0.0000	0.9970	0.0070	0.0030
Quadratic SVM	0.9969	0.0039	0.0031	1.0000	0.0000	0.0000	0.9980	0.0060	0.0020
Cubic SVM	0.9964	0.0077	0.0036	1.0000	0.0000	0.0000	0.9960	0.0070	0.0040
Medium Tree	0.9878	0.0183	0.0122	0.9995	0.0021	0.0005	0.9910	0.0222	0.0090
Bilayered NN	0.9975	0.0010	0.0025	1.0000	0.0000	0.0000	0.9995	0.0050	0.0005

5.1. Comparative *Analysis*

Finally, we also evaluated our results with the state-of-the-art techniques performed for lung cancer classification on different types of images. The comparison as shown in Table 6, presents the proposed technique's accuracy improvement.

Table 6. State-of-the-art Technique Comparison with Proposed Methodology

Paper	Dataset	Type of Images	Results
Anjum, S., et al. [18]	LC25000	Histopathological Images	97%
Uddin, J. J. D., et al. [23]	LC25000	15000 Histopathological Images	95.4%
Kumar, A., et al. [24]	LC25000	Histopathological Images	98.92%
Proposed Methodology	**LC25000**	**Histopathological Images**	**99.80%**

6. Conclusion & Future Work

The conventional method of a pathologist using histopathological imaging to diagnose lung cancer is laborious and prone to mistakes. In this paper, to address this issue, an automated Histopathological imaging-based technique is proposed. A dataset of histopathology images of lung cancer is gathered from LC25000, which consists of three different classes of lung cancer: Adenocarcinoma, Benign, and Squamous Cell Carcinoma. The EfficientNetB3 is a transfer learned over these images, and the features are obtained from the second-to-last layer, or the dropout layer of the model. Different classifiers then use this feature vector to observe their performance. The results show that 0.9980 accuracy is achieved by the proposed method for Bilayered NN. In the future, we will reduce the feature vector dimensions by applying different optimization techniques using different publicly available datasets.

Funding: This research received no external funding.

References

1. Islami F, Goding Sauer A, Miller KD, Siegel RL, Fedewa SA, Jacobs EJ, et al. Proportion and number of cancer cases and deaths attributable to potentially modifiable risk factors in the United States. 2018;68(1):31-54.
2. Sung H, Ferlay J, Siegel RL, Laversanne M, Soerjomataram I, Jemal A, et al. Global cancer statistics 2020: GLOBOCAN estimates of incidence and mortality worldwide for 36 cancers in 185 countries. CA: a cancer journal for clinicians. 2021;71(3):209-49.
3. Kratzer TB, Bandi P, Freedman ND, Smith RA, Travis WD, Jemal A, et al. Lung cancer statistics, 2023. 2024;130(8):1330-48.
4. Siegel RL, Kratzer TB, Giaquinto AN, Sung H, Jemal AJC. Cancer statistics, 2025. 2025;75(1):10.
5. Org WH. Cancer: World Health Organization (WHO); 2025 [Available from: https://www.who.int/news-room/fact-sheets/detail/cancer.
6. Ochoa-Ornelas R, Gudiño-Ochoa A, García-Rodríguez JA, Uribe-Toscano SJHA. A robust transfer learning approach with histopathological images for lung and colon cancer detection using EfficientNetB3. 2025;7:100391.
7. Cheng C, Li Y, Wu FJJoRR, Sciences A. Application value of early lung cancer screening based on artificial intelligence. 2024;17(3):100982.
8. Abbas S, Asif M, Rehman A, Alharbi M, Khan MA, Elmitwally NJH. RETRACTED: Emerging research trends in artificial intelligence for cancer diagnostic systems: A comprehensive review. 2024;10(17).
9. Luqman Ahmed MMI, Hamza Aldabbas, Shehzad Khalid, Yasir Saleem & Saqib Saeed. Image data practices for Semantic Segmentation of Breast Cancer using Deep Neural Network. Journal of Ambient Intelligence and Humanized Computing. 2023;14:15227–43, .
10. Chen H-Y, Su C-Y, editors. An enhanced hybrid MobileNet. 2018 9th International Conference on Awareness Science and Technology (iCAST); 2018: IEEE.
11. Zhu Y, Newsam S, editors. Densenet for dense flow. 2017 IEEE international conference on image processing (ICIP); 2017: IEEE.
12. Swapna M, Sharma YK, Prasadh BJIJRTE. Cnn architectures: Alex net, le net, vgg, google net, res net. 2020;8(6):953-60.
13. Sengupta A, Ye Y, Wang R, Liu C, Roy KJFin. Going deeper in spiking neural networks: VGG and residual architectures. 2019;13:95.
14. Alom MZ, Taha TM, Yakopcic C, Westberg S, Sidike P, Nasrin MS, et al. The history began from alexnet: A comprehensive survey on deep learning approaches. 2018.
15. Jiang X, Hu Z, Wang S, Zhang YJC. Deep learning for medical image-based cancer diagnosis. 2023;15(14):3608.
16. Batool A, Byun Y-CJIa. Lightweight EfficientNetB3 model based on depthwise separable convolutions for enhancing classification of leukemia white blood cell images. 2023;11:37203-15.
17. Borkowski AA, Bui MM, Thomas LB, Wilson CP, DeLand LA, Mastorides SMJapa. Lung and colon cancer histopathological image dataset (lc25000). 2019.
18. Anjum S, Ahmed I, Asif M, Aljuaid H, Alturise F, Ghadi YY, et al. Lung cancer classification in histopathology images using multiresolution efficient nets. 2023;2023(1):7282944.
19. Li M, Ma X, Chen C, Yuan Y, Zhang S, Yan Z, et al. Research on the auxiliary classification and diagnosis of lung cancer subtypes based on histopathological images. 2021;9:53687-707.
20. Singh O, Kashyap KL, Singh KKJSCS. Lung and colon cancer classification of histopathology images using convolutional neural network. 2024;5(2):223.
21. Mahmud MR, Fardin H, Siddiqui MIH, Sakib AH, Sakib AAJIJoS, Archive R. Hybrid deep learning for interpretable lung cancer recognition across computed tomography and histopathological imaging modalities. 2025;15(1):1798-810.

22. Adnan Shafait Ali MMI, Ali Haider Khan, Noureen Hameed, & Sumayya Bibi. Lung Cancer Detection Using Convolutional Neural Networks from Computed Tomography Images. Journal of Computing & Biomedical Informatics. 2023;6(1):133–43.
23. Uddin JJD. Attention-based DenseNet for lung cancer classification using CT scan and histopathological images. 2024;8(2):27.
24. Kumar A, Vishwakarma A, Bajaj VJCM, Biomedicine Pi. ML3CNet: Non-local means-assisted automatic framework for lung cancer subtypes classification using histopathological images. 2024;251:108207.
25. Li Z, Zhang J, Tan T, Teng X, Sun X, Zhao H, et al. Deep learning methods for lung cancer segmentation in whole-slide histopathology images—the acdc@ lunghp challenge 2019. 2020;25(2):429-40.
26. Nafea AA, Ibrahim MS, Shwaysh MM, Abdul-Kadhim K, Almamoori HR, AL-Ani MMJWJoC, et al. A deep learning algorithm for lung cancer detection using EfficientNet-B3. 2023;2(4):68-76.
27. Deng J, Dong W, Socher R, Li L-J, Li K, Fei-Fei L, editors. Imagenet: A large-scale hierarchical image database. 2009 IEEE conference on computer vision and pattern recognition; 2009: Ieee.
28. Torrey L, Shavlik J. Transfer learning. Handbook of research on machine learning applications and trends: algorithms, methods, and techniques: IGI Global Scientific Publishing; 2010. p. 242-64.